# Cosmic ray air showers in the knee energy region

S SANYAL

High Energy and Cosmic Ray Centre, North Bengal University, Darjeeling 734 430, India
Email: ssanyalcr@hotmail.com

**Abstract.** The cosmic ray extensive air showers in the knee energy region have been studied by the North Bengal University array. The differential size spectra at different atmospheric depths show a systematic shift of the knee towards smaller shower size with the increase in atmospheric depth. The measured values of spectral indices at below and above the knee are $-2.45 \pm 0.03$ and $-2.91 \pm 0.05$ respectively. Measurements at different atmospheric depths correspond to the same values within the error limits both for below and above the knee. The present experimental results have been compared with similar such experiments.

## 1. Introduction

The study of the origin and propagation of cosmic rays need a detailed study of the primary energy spectrum. Direct measurements of the energy spectrum have been carried out up to about 1 PeV by balloon and satellite borne detectors [1–6] flown to the top of the atmosphere. At higher energies the low flux of cosmic particles limits to the extensive air shower (EAS) technique that is the only feasible experimental method by which the energy spectrum can be derived from different EAS observables. From various measurements it is established that the primary energy spectrum can be well represented as a power law. The steepening of the spectrum at primary energy of a few PeV (the so-called 'knee') was confirmed by many experiments at different atmospheric depths after its first detection from the study of EAS size spectra at sea level [7]. However, the cause of the sudden change in the exponent of the power law energy spectrum has not been clearly understood yet. At present some high precision EAS experiments are in operation to register showers initiated by primaries with energy $10^{14}$ eV and above at different atmospheric depths throughout the world: the EAS-TOP experiment (INFN National Gran Sasso Laboratories, Campo Imperatore, Italy) at 820 g·cm$^{-2}$ [8], the HEGRA experiment (Canary Island, La Palma, Germany) at 800 g·cm$^{-2}$ [9], the KASCADE experiment (Karlsruhe, Germany) at 1020 g·cm$^{-2}$ [10], the ANDYRCHY experiment (Russia) at 800 g·cm$^{-2}$ [11], the MAKET-ANI installation (Mt. Aragats, Armenia) at 700 g·cm$^{-2}$ [12], the GRAPES experiment (Ooty, India) at 800 g·cm$^{-2}$ [13] etc. The simulation of EAS including full detectors' response

used to be carried out in the frame of CORSIKA code [14] using different hadronic inter-action and propagation models: HDPM [15], HEMAS [16], VENUS [17], SIBYLL [18], DPMJET [19], QGSJET [20] etc. Despite the overall improvement of experimental and analytical techniques in EAS analysis, the physical interpretation of the problem on the knee region is far from being solved. None of the hadron interaction models can describe all the observables in a consistent way to obtain a final result on mass composition and energy spectrum of the primary cosmic rays. In this paper a study of the characteristics of the air shower size spectra at the knee region of the primary energy spectrum observed at different atmospheric depths by the present experiment has been made. The results have also been compared with similar such results.

## 2. Experiment

The EAS array is located at the North Bengal University (NBU) Campus, Darjeeling, India (latitude $26°42'$ N, $88°21'$ E, atmospheric depth 1000 g·cm$^{-2}$). At present the array covers an area of $\sim$2000 m$^2$ consisting of 21 electron density sampling plastic scintillation detectors, eight fast timing scintillation detectors and two muon magnet spectrographs. Each scintillation detector has been built up with a 50 cm $\times$ 50 cm $\times$ 5 cm plastic scintillator (NE102A) block fixed at the upper end of an inverted pyramidal shaped light tight box made of galvanized iron sheet which is viewed by a photomultiplier (PM) tube from the lower end. For the electron density measuring detectors any one of Dumont 6364/RCA 5819/Philips XP2050 PM tubes are used while Philips XP2020 fast PM tubes (rise time $\sim$2 nS) are used for the fast timing detectors. The array has a circular symmetry with $\sim$8 m spacing between the detectors. Two solid iron magnet spectrograph units under concrete shielding ($\sim$1100 g·cm$^{-2}$) are also operated in association with the EAS array [21,22]. The construction and geometry of the apparatus sets the maximum detectable momentum of 500 GeV/c with the threshold of 2.5 GeV/c for the detection of EAS associated muons. The data is recorded under an EAS trigger generated by the four-fold coincidence of the fast timing detectors located around the center of the array. The trigger corresponds to passage of at least one particle in each of these four detectors. This fast coincidence generates the reference time for the time delay measurements by the fast timing detectors. To digitize the relative arrival time delay between the timing detectors, the LeCroy 2228A time-to-digital converter (TDC) module is used. The analog pulses from the electron density measuring detectors are digitized using the 8-bit analog-to-digital converters (ADC 0809). The digitized information from the entire ADC and the TDC channels along with the event time are sent to the memory units (62256) for subsequent transfer to the interfaced computer for permanent storage.

## 3. Data analysis and error estimation

The density of charged particles recorded in each detector is calculated from the ADC readings using the values of the average single particle pulse height and the area of the detector. The initial estimation of the core location $(X_0, Y_0)$ is made by taking the center of gravity of the density distribution as

$$X_0 = \frac{\sum \rho_i x_i}{\sum \rho_i} \quad \text{and} \quad Y_0 = \frac{\sum \rho_i y_i}{\sum \rho_i},$$

where $\rho_i$ is the density recorded at the $i$th detector located at $(x_i, y_i)$.

These recorded electron densities are corrected for transition effect in plastic scintillator [23]. The estimation of the EAS parameters are performed by means of a chi-square minimization routine using gradient search technique in which the recorded electron densities are compared with the theoretical NKG lateral distribution function [24]:

$$\rho(N_e, S, r) = C(S) \left( \frac{N_e}{r_0^2} \right) \left( \frac{r}{r_0} \right)^{S-2} \left[ 1 + \left( \frac{r}{r_0} \right) \right]^{S-4.5}, \tag{1}$$

where $\rho(N_e, S, r)$ is the density of the shower particles at a distance $r$ from the shower core of size $N_e$ and age $S$ with $r_0$ as the Moliere radius.

The error $(\sigma)$ in measuring the number of particles by the scintillation detectors is shown in figure 1. The radial variation of the shower age, its error estimates and unbiasness in the shower core selection had been discussed previously [25,26] in detail. To calculate the accuracy in the determination of shower size, the average number of particles in each detector is calculated by the NKG formula (eq. (1)) for a given $N_e, S$ and $(X_0, Y_0)$. The individual densities are fluctuated over the error estimated in figure 1. The trigger condition is imposed on these fluctuated showers for selection. The selected showers are again reconstructed through the same computer routine used for the estimation of the EAS parameters. The difference between the input size and the reconstructed size gives the error in the determination of shower size. The percent error thus obtained in size estimation is shown in figure 2 as a function of $N_e$. The systematic uncertainties in the measurements of the shower parameters are: $\pm 12\%$ in size, $\pm 8\%$ in age and $\pm 1.5$ m in core location, for showers whose cores hit within the area of $>95\%$ detection efficiency (described in §4).

The arrival direction of the shower front is estimated by minimizing the quantity $\chi^2$ defined as
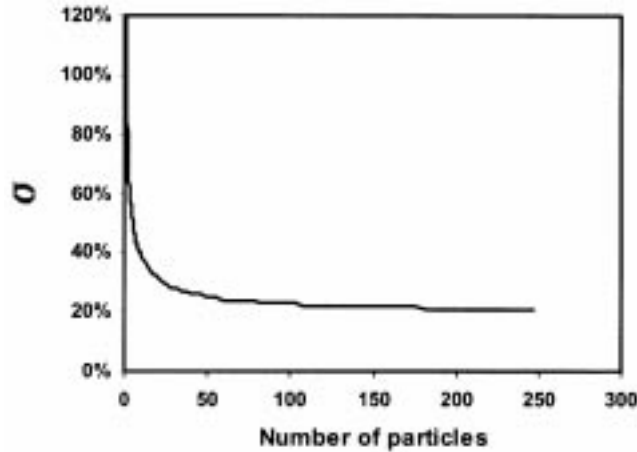


**Figure 1.** The error in the measurement of the number of particles by scintillation detectors of the array.
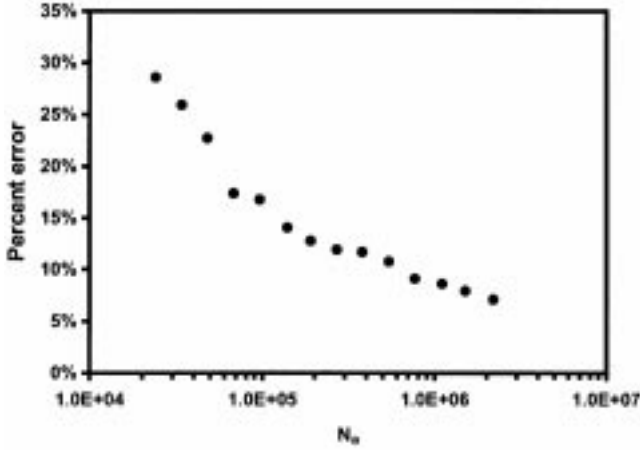
**Figure 2.** Per cent error in the shower size measurement as a function of $N_e$.

$$\chi^2 = w_i[lx_i + my_i + nz_i + c(t_0 - t_i)]^2, \tag{2}$$

where $(x_i, y_i, z_i)$ are the coordinates of the $i$th timing detector, $(l, m, n)$ are the direction cosines of the shower axis, $t_i$ is the actual arrival time measured at that detector, $t_0$ is the time at which the shower front passes through the origin of the coordinate system, $c$ is the velocity of the shower front and $w_i$ is the statistical weight factor defined as

$$w_i = (\sigma_{\text{inst}}^2 + \sigma_{\text{dsk}}^2)^{-1}, \tag{3}$$

where $\sigma_{\text{inst}}$ is the instrumental uncertainty and $\sigma_{\text{dsk}}$ is the uncertainty due to finite thickness of the EAS disk [27], which is dependent on shower parameters. The instrumental uncertainty is measured in the present experiment as, $\sigma_{\text{inst}} = 1.5$ ns. In the analysis, the plane shower front has been assumed neglecting its small but finite curvature [28], which does not result in a large error in our detection range. The fitted shower front is not constrained to pass through any detector since the parameter $t_0$ is taken as a free parameter. For the determination of the actual arrival time, the arrival times recorded by the timing detectors are corrected for time offsets [29] which arise due to unequal length and manufacturing differences of timing pulse cables, differences in transit times of the PM tubes and differences in electronic propagation delays in different timing channels. The resolutions in the arrival angle determination have been measured by the divided array method [30–32], which are 1.2° in zenith (z) and 1.8° in azimuth (A) for vertically incident showers.

## 4. Results

For the construction of the size spectrum the showers whose cores hit within the area of >95% detection efficiency are selected. To determine the detection efficiency in terms of radial distance from the array center, the whole array is divided into several concentric annular rings using its azimuthal symmetry. The shower core is randomly selected in a particular annular ring for a given shower size, age and zenith angle. The densities in

different detectors are calculated using the NKG function (eq. (1)) with $\cos(z)$ reduction of core distance. These individual densities are then fluctuated with the total error as standard deviation assuming the fluctuation as Gaussian in nature. Using these fluctuated densities the selection criteria for a particular size group is imposed to check whether the shower is selected or not. The calculation is repeated many times to attain statistical significance for a particular $N_e, S$ and $z$ in a particular annular ring. The fraction of showers selected out of the total number of generated showers gives the efficiency of the particular annular ring. The whole procedure is repeated for different values of $N_e, S, z$ and for different annular rings. The variation of >95% efficient area in terms of radial distance from the center of the array $(R_{95})$ is shown in figure 3 as a function of $N_e$ for different zenith angles.

In the present study the shower size spectra are constructed for different angular bins in such a way that the atmospheric thickness increases by a constant amount ($\sim$100 g·cm$^{-2}$). The showers are classified into different size bins for a particular zenith angle bin in the whole detection range $(10^{4.25}$–$10^{6.45})$. Size bins are formed by successive multiplication by $\sqrt{2}$ starting from the initial size of $10^{4.3}$. The $R_{95}$ is determined for the lower size limit of each bin. The differential shower size spectra for five different atmospheric depths are shown in figure 4. To emphasize the change in slope in the size region $10^5$–$10^6$ particles, the experimentally measured differential fluxes $(dI/dN_e)$ are multiplied by $N_e^{2.5}$. The vertical bars represent statistical errors only. Figure 5 shows the variation of the spectral indices with atmospheric depth for the electron size spectra below and above the knee. Besides the present experimental data the figure also includes the experimental results of the KASCADE [33], the MAKET-ANI [12] and the EAS-TOP [34]. The weighted average values of the spectral indices below and above the knee are, $\gamma_1 = -2.45 \pm 0.03$ and $\gamma_2 = -2.91 \pm 0.05$ respectively, calculated from the present experimental data. Though the measurements have been made at different atmospheric depths, the spectral indices correspond to single values within the error limits both below and above the knee. The fitted knee positions are plotted as a function of atmospheric depth in figure 6. The figure also includes the KASCADE and the EAS-TOP data. The shower size becomes smaller with the increase in atmospheric depth. The experimental data obtained from different experiments follow the same trend.
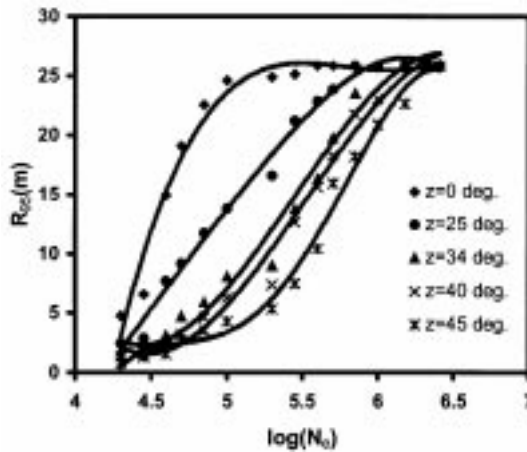


**Figure 3.** Variation of the radius $(R_{95})$ of >95% detection efficiency with shower size for different zenith angles.
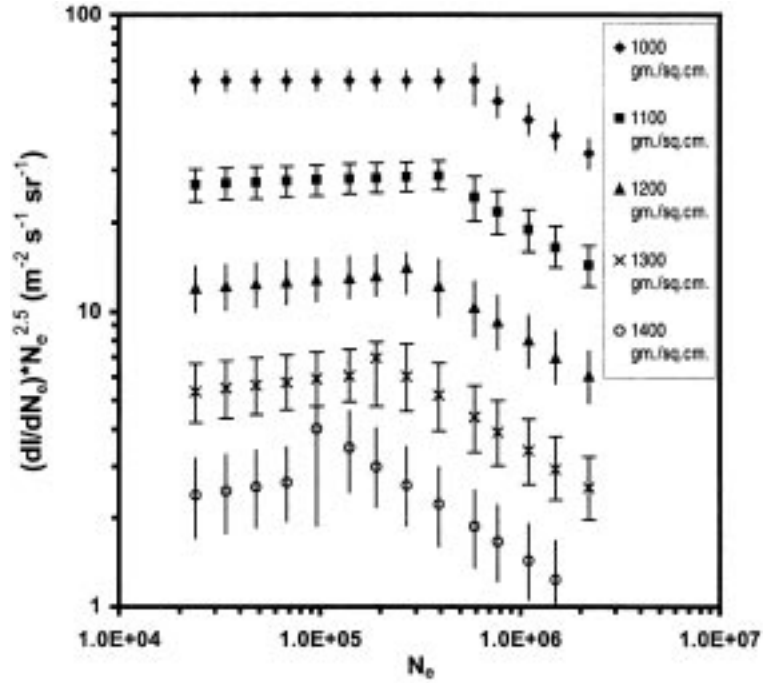
**Figure 4.** The differential size spectra measured at different atmospheric depths.

## 5. Discussion

Theoretical explanation of the knee deals with a number of possibilities. The assumption of a change of the source of cosmic rays and the effects of a change of the hadronic in- teraction mechanisms around the knee energy are more popular than other astrophysical reasons like the effects of the features of the cosmic ray transport through the interstellar medium. Nikolsky [35] suggested that changing high-energy interaction characteristics in the earth's atmosphere might cause the knee. The production of a new type of heavy particle in the first interaction may result in a break in the spectrum. The 'single source model' proposed by Earlykin and Wolfendale [36] assumed that a shock wave generated by a recent supernova explosion at a distance of a few hundred pc from the solar system currently propagated causing distinct peaks of elemental groups in the energy spectrum. A more recent explanation by Wigmans [37] assumed that the inverse beta decay of protons with relic neutrinos could destroy protons, the kinematic channel of which is open around the knee energy corresponding to an electron neutrino mass of 0.4 eV approximately. The observed systematic shift of the knee towards smaller shower size as the depth increases is due to shower attenuation which is in agreement with expectation for its appearance at fixed primary energy [33]. The present experimental results follow the same trend as observed by the KASCADE, the MAKET-ANI and the EAS-TOP experiments. The measurements of the spectral indices at different atmospheric depths correspond to single values both be- low and above the knee. Although there is an indication of slow increase in the exponent
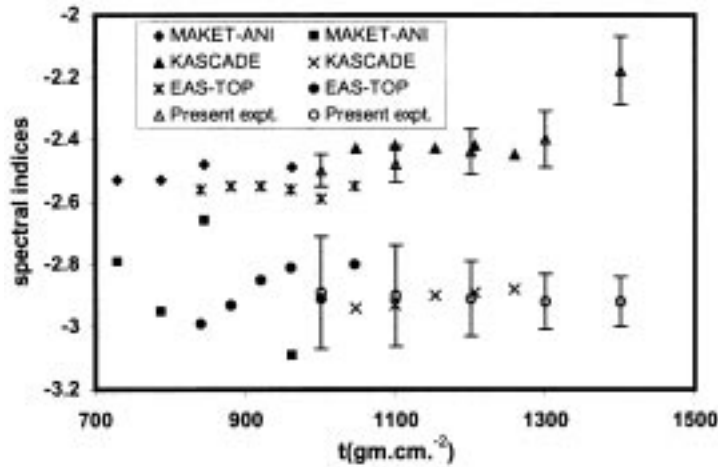
**Figure 5.** Variation of the spectral indices with atmospheric depth below and above the knee position.
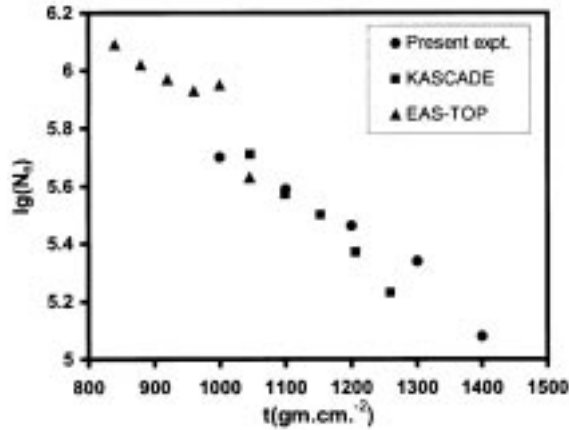


**Figure 6.** Position of the knee as a function of atmospheric depth.

of the power law energy spectrum up to the knee energy level when compared with similar such measurements (figure 5) more investigations are necessary before making a conclusive remark. The almost constant exponent above the knee may be an indication of either there is a single cosmic ray source or the sources that contribute to the cosmic rays above the knee energy level have identical energy spectra. A detailed knowledge of the chemical composition and the energy spectra of the cosmic ray primaries are necessary to solve the problem of the origin of the 'knee'.

## References

[1] V V Akimov, N L Grigorov, I D Rapoport, V Ye Nesterov, I A Savenko, G A Skuridin and A F Titenkov, *Geomagn. Aeron.* **11**, 327 (1971)

[2] V K Balasubrahmanyan and J F Ormes, *Astrophys. J.* **186**, 109 (1973)

[3] E Juliusson, *Astrophys. J.* **191**, 331 (1974)

[4] J A Lezniak and W R Webber, *Astrophys. J.* **223**, 676 (1978)

[5] A V Apanasenko *et al*, RUNJOB collaboration, *Proc. 26th Int. Cosmic Ray Conf. Salt Lake City* **3**, 163 (1999); **3**, 167 (1999)

[6] K Asakimori *et al*, JACEE collaboration, *Astrophys. J.* **502**, 278 (1998)

[7] G B Khristiansen and G V Kulikov, *Nuovo. Cimento Suppl.* **8**, 742 (1958)

[8] M Aglietta *et al*, EAS-TOP collaboration, *Nucl. Instrum. Methods* **A336**, 310 (1993)

[9] A Karle *et al*, HEGRA collaboration, *Astrop. Phys.* **3**, 321 (1995)

[10] H O Klages *et al*, KASCADE collaboration, *Nucl Phys.* (Proc. Suppl.) **B52**, 92 (1997)

[11] A E Chudakov, V B Petkov, V Ya Poddubny and A V Voevodsky, *Proc. 25th Int. Cosmic Ray Conf.* Durban, **6**, 173 (1997)

[12] A Chilingarian, G Hovsepyan, G Gharagyozyan, S Kazaryan, L Melkumyan, S Sokhoyan, E A Mamidjanyan, S I Nikolsky and V A Romakhin, ANI collaboration, *Proc. 26th Int. Cosmic Ray Conf.*, *Salt Lake City*, **1**, 240 (1999)

[13] Y Hayashi, Y Aikawa, N V Gopalakrishnan, S K Gupta, N Ito, S Kawakami, D K Mohanty, K C Ravindran, K Sasaki, M Sasano, K Sivaprasad, B V Sreekantan, H Tanaka, S C Tonwar and K Viswanathan, *Proc. 26th Int. Cosmic Ray Conf.*, *Salt Lake City* **1**, 276 (1999)

[14] D Heck, KASCADE collaboration, *Proc. 25th Int. Cosmic Ray Conf.*, *Durban*, **6**, 245 (1997)

[15] J N Capdevielle, *J. Phys.* **G15**, 909 (1989)

[16] C Forti, H Bilokon, B d'Ettorre Piazzoli, T K Gaisser, L Satta and T Stanev, *Phys. Rev.* **D42**, 11, 3668 (1990)

[17] K Werner, *Phys. Rep.* **232**, 87 (1993)

[18] R S Fletcher, T K Gaisser, P Lipari and T Stanev, *Phys. Rev.* **D50**, 9, 5710 (1994)

[19] J Ranft, *Phys. Rev.* **D51**, 1, 64 (1995)

[20] N N Kalmykov, S S Ostapchenko and A I Pavlov, *Nucl. Phys.* (*Proc. Suppl.*), **B52**, 17 (1997)

[21] S Sanyal, D K Basak, N Chaudhuri, S K Sarkar and N Mukherjee, *Proc. 21st Int. Cosmic Ray Conf.*, *Adelaide*, **9**, 130 (1990)

[22] D K Basak, S K Sarkar, N Mukherjee, S Sanyal, B Ghose and N Chaudhuri, *Can. J. Phys.* **68**, 41 (1990)

[23] K Asakimori, T Hata, T Maeda, N Nishijima, Y Toyoda, K Kamamoto, M Yoshida, T Kameda and K Mizushima, *Proc. 17th Int. Cosmic Ray Conf.*, *Paris*, **11**, 301 (1981)

[24] K Greisen, *Ann. Rev. Nucl. Sci.* **10**, 63 (1960)

[25] S Sanyal, B Ghosh, S K Sarkar, A Bhadra, A Mukherjee and N Chaudhuri, *Aust. J. Phys.* **46**, 589 (1993)

[26] S Sanyal, B Ghosh, S K Sarkar, A Mukherjee, A Bhadra and N Chaudhuri, *Proc. 23rd Int. Cosmic Ray Conf.*, *Calgary*, **4**, 343 (1993)

[27] J Linsley, *Proc. 19th Int. Cosmic Ray Conf.*, *La Jolla*, **3**, 461 (1985)

[28] P Bassi, G Clark and B Rossi, *Phys. Rev.* **92**, 441 (1953)

[29] S Sanyal, *A study of sensitivity of different high energy interaction models by the cosmic ray extensive air shower technique at the energy level of $10^{14}$ eV*, Ph.D. thesis (North Bengal University, 1995)

[30] S Sinha, B S Acharya, P N Bhat, S G Khairatkar, M R Rajeev, M V S Rao, K Sivaprasad, B V Sreekantan, P R Vishwanath and K Viswanathan, *Proc. 21st Int. Cosmic Ray Conf.*, *Adelaide*, **2**, 51, 126 (1990)

[31] B S Acharya, P N Bhat, A V John, S G Khairatkar, B K Nagesh, M R Rajeev, K S Rao, M V S

Rao, A Reddy, S Sinha, K Sivaprasad, A J Stanislaus, B L Venkateshmurthy, P R Vishwanath, P Unnikrishnan and S S Upadhya, *Proc. 23rd Int. Cosmic Ray Conf.*, *Calgary*, **1**, 212 (1993)

[32] B S Acharya, P N Bhat, A V John, S G Khairatkar, B K Nagesh, M R Rajeev, K Shobha Rao, M V S Rao, A Reddy, S Sinha, K Sivaprasad, A J Stanislaus, B L Venkateshmurthy, P R Vishwanath, K Viswanathan, P Unnikrishnan and S S Upadhya, *J. Phys.* **G19**, 1053 (1993)

[33] R Glasstetter *et al*, KASCADE collaboration, *Proc. 25th Int. Cosmic Ray Conf.*, *Durban*, **6**, 157 (1997)

[34] M Aglietta *et al*, EAS-TOP collaboration, *Proc. 26th Int. Cosmic Ray Conf.*, *Salt Lake City*, **1**, 230 (1999)

[35] S I Nikolsky, *Nucl. Phys.* (*Proc. Suppl.*) **A39**, 228 (1995)

[36] A D Earlykin and A W Wolfendale, *J. Phys.* **G23**, 979 (1997)

[37] R Wigmans, *Nucl. Phys.* (*Proc. Suppl.*) **85**, 305 (2000)